minerals

MDPI

Article

Research on Enhancing Copper-Ammonia-Thiosulfate Eco-Friendly Gold Leaching by Magnetization of Lixiviant Solution and Their Kinetic Mechanism

Zhengyu Liu [1], Jue Kou [1,*], Lipeng Fan [2], Weibin Zhang [3], Jie Tian [4], Chunbao Sun [1], Qiang Li [3], Jiubo Liu [3], Chengjun Xing [3] and Guanhua Li [3]

[1] School of Civil and Resources Engineering, University of Science and Technology Beijing, 30 Xueyuan Road, Beijing 100083, China; zhengyuliu1998@163.com (Z.L.); suncb@ustb.edu.cn (C.S.)
[2] Ansteel Group Mining Company Ltd., 39 219 Road, Anshan 114010, China; fanlipeng19911115@163.com
[3] China National Gold Group Inner Mongolia Taiping Mining Co., Ltd., 42 Keerlun Road, Hulun Buir 021399, China; weibinz@chinagoldintl.com (W.Z.); liqiang@chinagoldintl.com (Q.L.); bobl@chinagoldintl.com (J.L.); chengjunx@chinagoldintl.com (C.X.); guanhual@chinagoldintl.com (G.L.)
[4] Engineering Company of Beijing General Research Institute of Mining and Metallurgy Technology Group, 22 Beixing Road, Beijing 100162, China; tianjie@bgrimm.com
* Correspondence: koujue@ustb.edu.cn

Abstract: In thiosulfate leaching of gold, the copper-ammonia complex serves as an oxidant and catalyst. This study examined the impact of magnetizing the copper-ammonia thiosulphate lixiviant solution on gold leaching from refractory oxidized ores. Magnetization reduced surface tension, improved wettability and infiltration, and enhanced the diffusion of leaching agents. It also increased dissolved oxygen content and boosted the catalytic efficiency of copper-ammonia complexes. These changes led to more efficient gold extraction, with column leaching showing a 4.74% improvement in extraction rates compared to non-magnetized methods and a 3.67% improvement over cyanide processes. These findings suggest that magnetized copper-ammonia thiosulphate lixiviant is a promising, environmentally friendly alternative to cyanide for refractory oxidized gold ores.

Keywords: copper-ammonia-thiosulfate lixiviant; gold leaching; magnetization treatment; surface tension; kinetic

check for updates

Citation: Liu, Z.; Kou, J.; Fan, L.; Zhang, W.; Tian, J.; Sun, C.; Li, Q.; Liu, J.; Xing, C.; Li, G. Research on Enhancing Copper-Ammonia-Thiosulfate Eco-Friendly Gold Leaching by Magnetization of Lixiviant Solution and Their Kinetic Mechanism. *Minerals* **2024**, *14*, 697. https://doi.org/10.3390/min14070697

Academic Editors: Richmond K. Asamoah, Ahmet Deniz Baş, George Blankson Abaka-Wood, Kali Sanjay and Jonas Addai-Mensah

Received: 26 June 2024
Revised: 2 July 2024
Accepted: 5 July 2024
Published: 8 July 2024

1. Introduction

Cyanidation presently stands as the predominant method for gold leaching in established industrial practices due to its notable efficiency and rapidity [1,2]. However, the considerable toxicity of cyanide presents significant risks, with potential leaks of cyanide leaching chemicals and tailings posing threats to human and animal lives in the vicinity as well as environmental safety [3]. While sealed reaction tanks can be employed for cyanide leaching in high-grade gold ores, low-grade refractory gold ores necessitate open heap leaching as the more economically viable approach [4]. Notably, the drawbacks associated with cyanidation become more pronounced in the context of open heap leaching for low-grade refractory gold ores. To mitigate the reliance on cyanide, various environmentally sustainable lixiviants [5–8] such as halogen [9–11], amino acids [12], and thiosulfate [13] have been developed. Among these, halogen and amino acids face challenges in large-scale industrial gold-bearing ore treatment due to factors like high costs, pollution concerns, and limited treatment scale [14]. Thiosulfate emerges as a promising cyanide alternative, tracing its origins back to the early 20th century when it was known as the Von Patera method [15,16]. Compared to cyanidation, thiosulfate-based leaching offers improved production safety and exhibits less sensitivity to impurities, making it better suited for treating complex gold ores containing carbonaceous, copper, and arsenic elements [17–19].

In an oxidizing environment, gold solubilization occurs via thiosulfate, leading to stable gold thiosulfate complexes including $AuS_2O_3^-$ and $Au(S_2O_3)_2^{3-}$ [20,21]. The latter, with a complexation stability constant reaching up to $10^{24.00}$, predominates among gold thiosulfate complexes [13]. The reaction between gold and thiosulfate under alkaline conditions is depicted in Equation (1).

$$4Au + 8S_2O_3^{2-} + 2H_2O + O_2 = 4[Au(S_2O_3)_2]^{3-} + 4OH^- \quad (1)$$

The development of copper-ammonia thiosulfate leaching systems has notably enhanced gold leaching efficiency. The copper-ammonia complex acts as an oxidant, reacting directly with gold and then oxidizing to form a copper-ammonia complex in the presence of oxygen. This complex can also function as a catalyst for the thiosulfate leaching reaction, as shown in Equations (2) and (3) [22].

$$Au + 5S_2O_3^{2-} + [Cu(NH_3)_4]^{2+} = [Au(S_2O_3)_2]^{3-} + 4NH_3 + [Cu(S_2O_3)_3]^{5-} \quad (2)$$

$$2[Cu(S_2O_3)_3]^{5-} + 8NH_3 + 0.5O_2 + H_2O = 2[Cu(NH_3)_4]^{2+} + 2OH^- + 6S_2O_3^{2-} \quad (3)$$

While copper-ammonia thiosulfate lixiviant solutions offer advantages such as stable gold complex formation, rapid leaching rates, non-toxicity, and reduced pollution, challenges persist, including high thiosulfate consumption, solution instability, complex components, and elevated leaching costs [23]. Various studies have explored enhancing gold leaching within copper-ammonia thiosulfate systems through approaches such as [24], electrolytic reduction [25], and ligand substitutions [26,27]. Among them, the use of ionic liquids instead of water solvents can significantly increase the conductivity of the gold leaching reaction medium and improve the electrochemical reaction process of gold leaching, but the ionic liquids are too expensive, which hinders its industrial-scale adoption.

Magnetization treatment of water has garnered attention for its ability to induce significant property changes, affecting parameters such as surface tension, viscosity, electrical conductivity, water molecule cluster size, and dissolved oxygen (DO) [28–32]. These changes have found applications in diverse fields such as coal mine dust suppression [33], crop growth [34], concrete manufacturing [35], and water pipe scale inhibition [36]. Pang [37] and Zhou [38] studied magnetization's impact on water surface tension, observing reductions of 7.28% and 6.33%, respectively, and concluded that magnetization mainly destroys hydrogen bonds between water molecules and reduces the cohesion of the solution. Amiri [39] confirmed this effect but noted an optimal magnetization duration, beyond which surface tension increased. Sronsri [40] examined molecular changes in magnetized water, highlighting disrupted hydrogen bonds and the formation of smaller water molecular groups, leading to increased hydrogen bonds outside the molecular group [41].

In the context of gold ore leaching, the wettability of the lixiviant agent on gold surfaces and the dissolved oxygen content in the solution are crucial factors influencing the contact of the lixiviant agent and gold and oxidation potential which in turn affects leaching efficiency. Moreover, the presence of paramagnetic molecules in the solution, aside from water, may also undergo changes under magnetic fields, affecting leaching reactions. Therefore, understanding how magnetization influences the gold-leaching process within copper-ammonia thiosulfate systems is imperative.

This study aims to investigate the impact of magnetization on the properties of copper-ammonia sodium thiosulfate lixiviant solutions, including surface tension, DO, wettability, and chemical activity, within the context of heap leaching from low-grade gold ores. The study also explores the enhanced effects of magnetization on reaction rates and kinetics in copper-ammonia sodium thiosulfate gold leaching through Quartz Crystal Microbalance with Dissipation (QCMD) and leaching kinetics tests. Additionally, a comparison is made between gold extraction rates using magnetized copper-ammonia sodium thiosulfate leach and sodium cyanide leach through column leaching tests.

2. Materials and Methods

2.1. Materials and Reagents

The gold foil utilized for the leaching kinetics test measures 5 mm × 5 mm × 0.1 mm, exhibiting a gold purity exceeding 99.99%. Simultaneously, the gold-plated quartz resonator employed in the QCMD test featured a gold layer approximately 100 nm thick, with a fundamental frequency of 15 MHz.

The refractory gold ore head sample was sourced from the Changshanhao gold mine and underwent crushing to achieve a fragment size of −10.0 mm. The primary mineral components of the sample include quartz, pyroxene, mica, feldspar, pyrrhotite, and pyrite.

The gold grade within the ore sample was determined to be 0.48 g/t, primarily comprising natural gold and silver gold ore. These gold minerals predominantly exist in fine-grained and micro-fine-grained forms, coexisting with gangue minerals like quartz and pyroxene. A minor proportion is found in symbiosis with pyrite, pyrrhotite, and other sulfide ores.

The results of the mineral phase analysis of gold, as depicted in Table 1, indicate that bare and semi-bare gold minerals constitute the dominant phase at 64.58%, followed by carbonate-encapsulated gold at 27.08%, with the remaining gold encapsulated within other minerals at 8.33%.

Table 1. Gold phase analysis results.

Gold Phase	Gross Gold	Bare and Semi-Bare Gold	Carbonate-Encapsulated Gold	Sulfides-Encapsulated Gold	Hematite-Encapsulated Gold	Quartz and Silicates-Encapsulated Gold
Content (g/t)	0.48	0.31	0.13	<0.1	<0.1	<0.1

The sodium thiosulfate, copper sulfate, and ammonia utilized in this study are analytical reagents. The method for preparing the lixiviant solution involves initially preparing the copper-ammonia complex solution, followed by combining it with the sodium thiosulfate solution. The proportion of copper sulfate, ammonia, and sodium thiosulfate in the prepared lixiviant solution is 5:35:1.

2.2. Experiments

2.2.1. Magnetization of Lixiviant Solution

The magnetization diagram of the lixiviant solution and the distribution of the magnetic field within the magnetizer (manufactured by Huate Magnet, Linqu, China) is depicted in Figure 1. The magnet within the magnetizer is constructed using N54 NdFeB permanent magnet material, generating a magnetic field strength of approximately 1.5 T. The length of the magnetic field spans 55 mm, and the inner diameter of the hose attached to the magnetizer measures 8.0 mm. The lixiviant solution is delivered into the magnetizer via a peristaltic pump. At a specific flow rate, a defined volume of lixiviant solution traverses the magnetic field within the magnetizer through the hose, becoming magnetized during the effective magnetization period. After undergoing several magnetization cycles, the entire lixiviant solution becomes fully magnetized. Two important magnetization parameters, namely effective magnetizing time and cycle times are calculated according to Equations (4) and (5).

$$\text{Effective magnetizing time} = \text{Flow rate}/\text{Magnetic feild length} \times \text{pipe cross} - \text{sectional area} \quad (4)$$

$$\text{Cycle times} = \text{Gross lixiviant solution volumn}/\text{Flow rate} \quad (5)$$

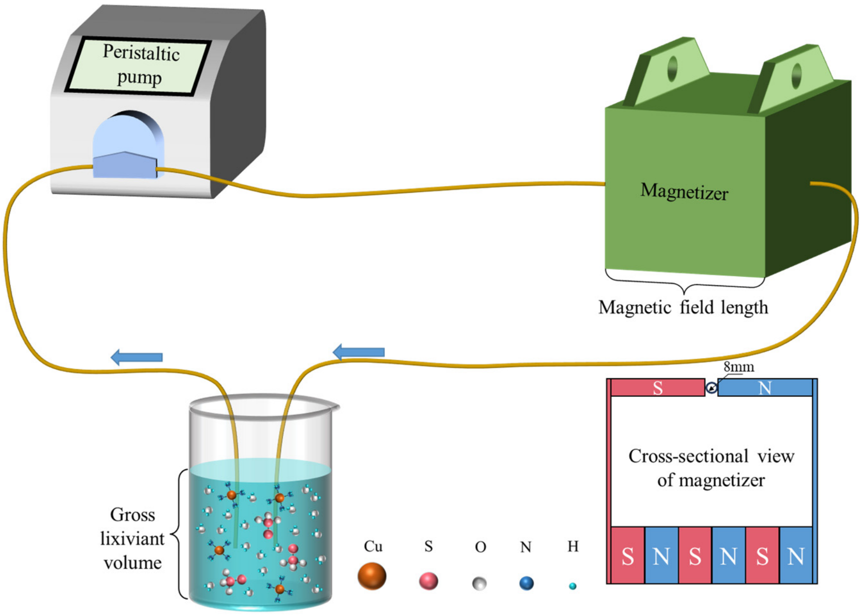

Figure 1. Magnetization process of lixiviant solution and cross-sectional view of magnetizer.

2.2.2. Column Leaching

The column leaching test replicates the operational dynamics of ore heap drip leaching. This simulation involves filling a plexiglass column with ore to conduct drip tests, mirroring a unit of the heap leaching process. Within the chamber, the dripping of lixiviant solution, ore leaching, and collection of precious liquids are executed, effectively emulating industrial heap-leaching production processes.

The test columns are custom-made Plexiglas cylinders, 0.15 m in inner diameter and 2.00 m in height, outfitted with valves at their base for ore column management. Lixiviant and leachate are stored separately in gelatinous drums. A metering pump delivers the leach solution to the column's top, with each column loaded with approximately 50 kg of ore samples.

Post-loading, the column undergoes treatment with sodium hydroxide lye at a pH of 10.5–11 to ensure thorough rinsing of the ore sample and cessation of lye discharge when pH stabilizes at 10.5–11. Stabilized sodium thiosulfate lixiviant solution is then dripped at an intensity of 6 L/(m^2·h) over a 20-day leaching period. Leachate is regularly sampled to assess volume, gold content, and thiosulfate concentration.

2.2.3. Leaching Rate Test Based on QCM-D

The experimental setup utilized in this study was the Q-sense E4 quartz crystal microbalance. Real-time measurements of the frequency (f) and energy dissipation (D) were conducted during the interaction of various sodium thiosulfate lixiviant solutions with gold, employing the QCM-D technique. The pH of the solutions was maintained at 11.5, and the reactions were carried out at a temperature of 25 °C.

To establish the equilibrium baseline, ultrapure water was initially pumped into the system at a flow rate of 100 μL/min. Subsequently, the frequency stabilization criteria were met (with fluctuations in f being less than 5 Hz), leading to the acquisition of the equilibrium baseline under the background solution. Following this, the lixiviant was introduced to initiate the lixiviant reaction, with a leaching duration set at 15 min.

The frequency change (Δf) was determined by subtracting the initial frequency of the gold resonator from the measured frequency (f) during the test. Similarly, the change in energy dissipation (ΔD) was calculated by subtracting the initial energy dissipation from the measured energy dissipation during the test. The Δf value was then converted into the change in mass (Δm) using the Sauerbrey model see Equation (6) [5].

$$\Delta f = \frac{-2\Delta m f^2}{A\sqrt{\mu_q \rho_q}} \tag{6}$$

where Δm is the mass change; A is the area of the gold-plated layer on the surface of the resonator where the leaching reaction occurs; μ_q is the shear modulus of the quartz crystal; ρ_q is the density of quartz crystal.

2.2.4. Contact Angle Test by Washburn Method

The change in contact angle of the magnetized lixiviant solution on the gold ore was assessed using the Washburn method. In the contact angle test, 2 g of powder was sampled and put into a glass tube with a filter at the bottom, the powder in the glass tube was vibrated 30 times, and then we hung the glass tube in the surface tensiometer hanging slot.

The bottom of the glass tube is in contact with the lixiviant solution. Due to the capillary effect, the lixiviant solution will be absorbed, and the mass of the glass tube and time meet Equation (7).

$$M^2 = t\frac{c\sigma\rho^2}{\eta} \times \cos\theta \tag{7}$$

where M^2 is the mass squared of the glass tube; t is the testing time; c is the ore powder capillary effect constant with a value of 0.156 mm^5 tested by hexyl hydride; σ is lixiviant solution surface tension; ρ is the solution density; η is solution viscosity, and θ is the contact angle.

2.3. Analytical Methods

The surface tension of the copper-ammonia sodium thiosulfate lixiviant solution was assessed using a K100-c type fully automatic surface tension meter manufactured by KRUSS. The Du Noüy ring method [42] was employed for measurement, with the instrument's range spanning from 0 to 200 mN/m and a resolution of 0.001 mN/m. The device boasts a repeatability error of no more than 1% for oscillometric values and offers temperature resolution down to 0.1 °C. To ensure data reliability, the automatic measurement procedure was set to conduct five measurements.

The sodium thiosulfate concentration in both the lixiviant solution and the precious liquid was determined via the iodometric method. Additionally, the concentration of the copper-ammonia complex in the solution was gauged using a UV spectrophotometer. To minimize fluctuations in the copper-ammonia complex concentration due to chemical reactions during scanning, the characteristic peak of the complex was fixed at 615 nm, with a scanning speed of 1200 nm/min, and each test was conducted in triplicate.

The gold grade in the run-of-mine (ROM) material was evaluated through the fire-assay atomic absorption method as per GB/T 20899.1-2019 standards [43]. For gold concentration in the solution, inductively coupled plasma-mass spectrometry (ICP-MS) was employed, following the atomic absorption method.

3. Results and Discussion

3.1. Lixiviant Solution Magnetization

The copper-ammonia-thiosulfate lixiviant solution within the magnetization device undergoes a continuous process of dynamic magnetization. Achieving a stable magnetization state requires a relaxation time, thus emphasizing the significant impact of the magnetic field's alternating frequency and the effective magnetization duration on the overall magnetization efficacy. Despite the magnetization device employing a constant magnetic field, it can be regarded as a dynamic magnetic field concerning the flowing solution. Consequently, the flow rate of the lixiviant solution within the apparatus, which reflects the frequency of magnetic field changes, and the magnetization duration, defined as the number of times the solution circulates through the magnetization device, emerge as the pivotal factors influencing magnetization effectiveness, particularly in terms of surface tension and dissolved oxygen (DO) levels within the solution.

3.1.1. Surface Tension

The experiment involved a magnetized lixiviant solution volume of 300 mL, a magnetization duration of 5 min, and various flow rates of the lixiviant solution through the magnetization device: 500, 750, 1000, 1250, and 1500 mL/min. The aim was to evaluate the lixiviant solution's surface tension post-magnetization under different flow rate conditions, depicted in Figure 2a. Hereafter, MT and BC represent the magnetization-treated group and blank control group, respectively.

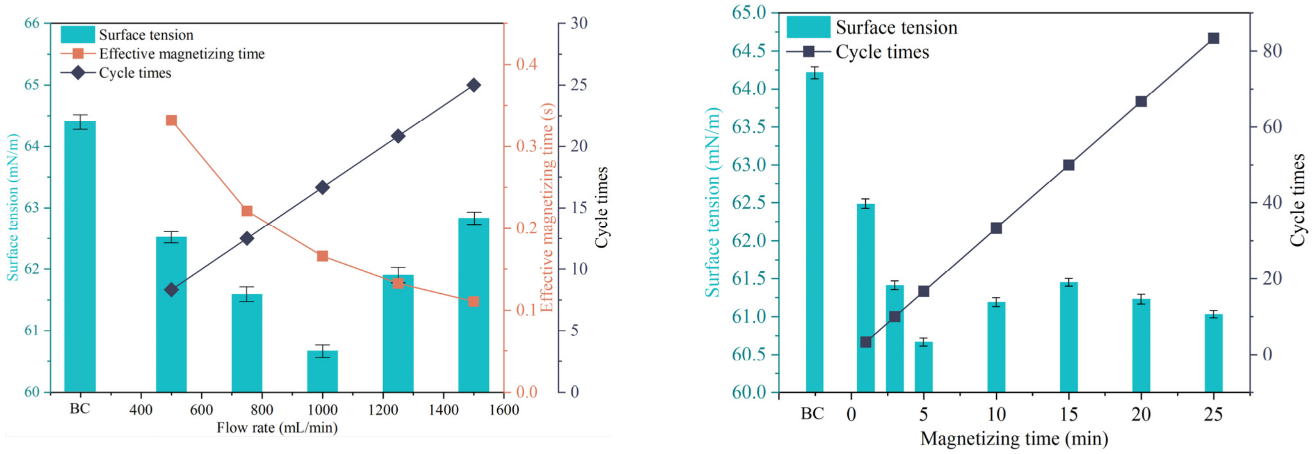

(**a**) (**b**)

Figure 2. Variation of surface tension: (**a**): varying lixiviant solution flow rate; (**b**): varying magnetizing time.

Figure 2a illustrates that as the flow rate increased, the effective magnetization time decreased continuously, and the number of magnetization cycles increased. Concurrently, the surface tension of the sodium thiosulfate lixiviant solution post-magnetization displayed a trend of initially decreasing and then increasing. For the non-magnetized sodium thiosulfate leaching solution, the surface tension stood at 64.38 mN/m. When the flow rate was 500 mL/min, corresponding to 8.33 cycles of the solution with an effective magnetization time of 0.33 s per cycle, the surface tension was reduced to 62.52 mN/m. Doubling the flow rate to 1000 mL/min increased the number of cycles to 16.67, with a corresponding reduction in effective magnetization time per cycle to 0.17 s. This resulted in the lowest surface tension of 60.67 mN/m, a decrease of 3.71 mN/m compared to the control group, representing a 5.76% reduction.

However, at a flow rate of 1500 mL/min, despite 25 cycles of the solution, the effective magnetization time per cycle decreased to 0.11 s, leading to a rebound in surface tension to 62.83 mN/m. Increasing turbulence due to the higher flow rate hindered sufficient magnetization of the sodium thiosulfate leaching solution, disrupting the magnetization state from the previous cycle. Moreover, heightened turbulence disturbed the initial magnetization state, contributing to decreased surface tension. Consequently, a flow rate of 1000 mL/min was determined as optimal for magnetizing the sodium thiosulfate leaching solution for gold extraction.

The surface tension of the lixiviant solution post-magnetization treatment was assessed by varying the magnetization time at intervals of 1, 3, 5, 10, 15, 20, and 25 min and maintaining a constant flow rate of 1000 mL/min, as depicted in Figure 2b.

Figure 2b illustrates that as the magnetizing time increased, so did the duration of the magnetization treatment cycle. Concurrently, the surface tension of the lixiviant solution after magnetization displayed a trend of initial reduction followed by slight fluctuations. For a magnetization time of 1 min, corresponding to 3.33 cycles of magnetization treatment, the surface tension decreased to 62.48 mN/m. Extending the magnetization time to 5 min resulted in the lowest surface tension of 60.67 mN/m, representing a 5.76% reduction. While the surface tension exhibited minor fluctuations with prolonged magnetization cycle times, the changes were not significant. Therefore, a magnetization time of 5 min was identified as the optimal duration for the magnetization cycle.

3.1.2. DO

The experiment maintained a constant flow rate of 1000 mL/min for the lixiviant solution while varying the magnetization time at intervals of 0, 5, 10, 15, 20, 25, 30, and 35 min, respectively. The dissolved oxygen (DO) content of the lixiviant solution was then measured under these varying magnetization time conditions, as depicted in Figure 3a.

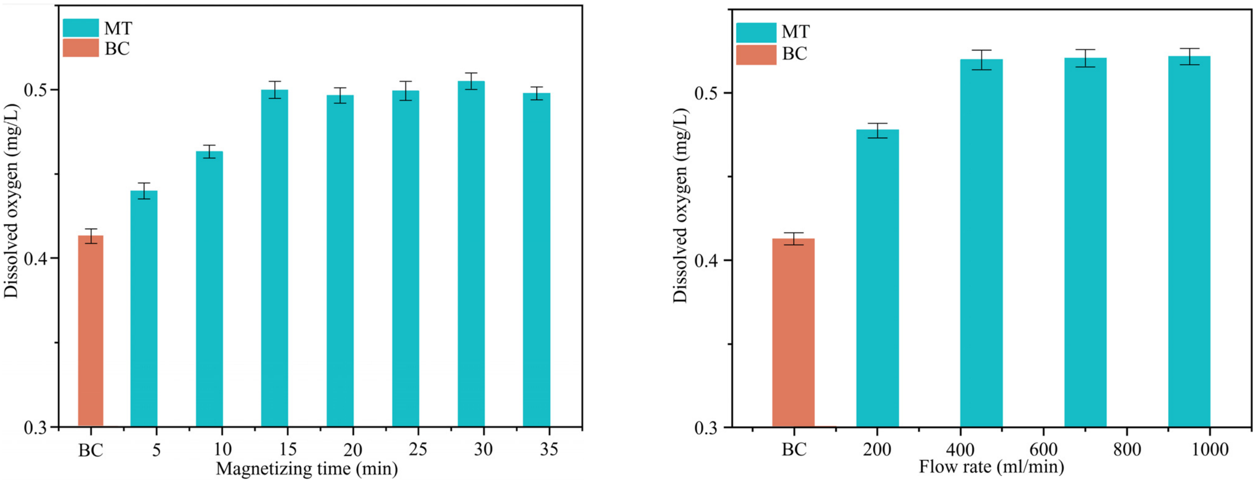

(**a**) (**b**)

Figure 3. Variation of Do content: (**a**) varying magnetizing time; (**b**) varying lixiviant solution flow rate.

It is pertinent to note that the DO content in water stood at 8.77 mg/L but Figure 3a shows that BC exhibits a lower DO content. This phenomenon arises from the reaction depicted in Equations (8) and (9), where thiosulfate reduces Cu(II) to Cu(I), and Cu(I) undergoes continuous oxidation to Cu(II) by oxygen, leading to oxygen consumption within the solution. Figure 3a shows that upon magnetization, the DO in the lixiviant solution initially rose before subsequently declining. For a magnetization time of 5 min, the DO measured 0.44 mg/L, marking a 0.03 mg/L increase compared to the BC. At 15 min of magnetization time, the DO peaked at 0.51 mg/L, reflecting a 0.09 mg/L increase over the BC. Beyond this duration, despite further magnetization time, the DO did not show a significant increase but rather declined gradually, indicating complete magnetization of lixiviant solution after 15 min.

$$S_2O_3{}^{2-} + 2Cu(NH_3)_4{}^{2+} \rightarrow 2Cu(S_2O_3)_2{}^{3-} + S_4O_6{}^{2-} + 8NH_3 \tag{8}$$

$$4Cu(S_2O_3)_2{}^{3-} + O_2 + 2H_2O + 16NH_3 \rightarrow 4Cu(NH_3)_4{}^{2+} + 8S_2O_3{}^{2-} + 4OH^- \tag{9}$$

The magnetization duration was fixed at 15 min, while the liquid flow rates were varied at 0, 300, 500, 1000, and 1200 mL/min, respectively, to investigate the DO content in the lixiviant solution under different flow rate conditions, as depicted in Figure 3b.

Figure 3b. illustrates a gradual increase in DO content with rising flow rates, albeit with a trend of diminishing returns. As the flow rate reached 500 mL/min, the DO content significantly rose to 0.49 mg/L which is attributed to that a higher flow rate results in more magnetization cycle times. As the flow rate increased to 750 mL/min, the DO content slightly increased to 0.52 mg/L which may be because of the heightened turbulence resulting from increased flow rates. Greater turbulence enhances the contact frequency between the oxygen-deficient solution and the surrounding air, leading to a slight increase in DO content.

Despite substantial oxygen consumption in the copper-ammonia sodium thiosulfate solution due to the reaction depicted in Equation (9), magnetization also contributed to a partial increase in DO levels within the solution.

3.2. Mechanism

3.2.1. Contact Angle

The contact angle, also known as Young's contact angle, is an important indicator for judging the wettability of liquids on solid surfaces. The smaller the contact angle, the more likely the liquid is to wet the solid surface. Hence, the contact angle of the lixiviant solution with gold ore powder, both before and after magnetization treatment, was assessed. The square of the mass of the glass tube containing the ore sample was plotted against time, and the contact angle of the lixiviant solution on the gold ore was calculated through fitting based on Equation (7), as depicted in Figure 4.

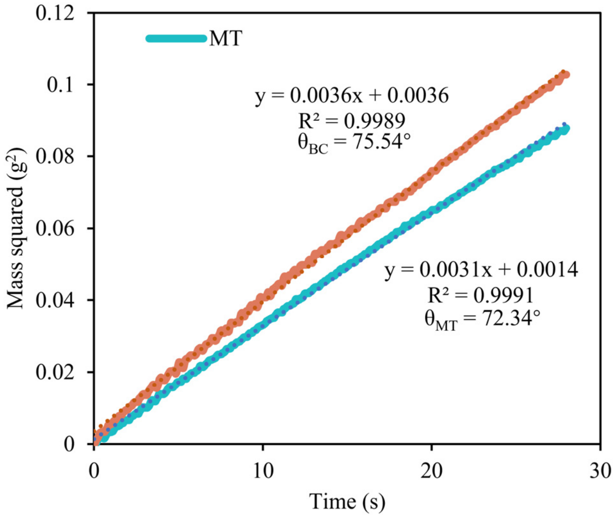

Figure 4. Contact angle test results.

Figure 4 reveals that, in terms of the slope of the fitted straight line, the non-magnetized lixiviant solution (BC) exhibits a steeper slope than the magnetized treatment (MT), indicating that magnetization significantly enhances the adsorption rate of the lixiviant solution onto the ROM. Additionally, the contact angle of the sodium thiosulfate lixiviant solution with gold ore powder decreased after magnetization, with a reduction of 3.20° in the powder contact angle post-magnetization. Moreover, the mass of the glass tube containing the magnetized sodium thiosulfate lixiviant solution group was greater compared to that of the non-magnetized group at the same time point, further supporting the notion that magnetization enhances the wettability of sodium thiosulfate lixiviant solution. This observation underscores the effectiveness of magnetization in reducing the contact angle between sodium thiosulfate lixiviant solution and gold ore, thereby improving the solution's wettability.

3.2.2. Chemical Reactivity

The reaction between copper ammonia and sodium thiosulfate to form copper thiosulfate compounds is a pivotal catalytic process within the copper-ammonia thiosulfate system, consuming a significant amount of copper ammonia complex as outlined in

Equation (8). This section delves into the impact of magnetization on the rate of this chemical reaction by evaluating the concentration of copper ammonia complex in the solution post-magnetization.

Initially, the fluctuations in copper-ammonia complex concentrations were assessed over resting periods before and after magnetization of lixiviant solutions with varying sodium thiosulfate concentrations, with results depicted in Figure 5a. Analysis of Figure 5a reveals that after an initial 5-min magnetization, the concentration of copper-ammonia complex in the magnetized and unmagnetized 0.15 mol/L groups was slightly higher at 0.0241 mol/L and 0.0246 mol/L, respectively, compared to the magnetized and unmagnetized 0.30 mol/L groups, which recorded 0.0287 mol/L and 0.0289 mol/L, respectively. This difference can be attributed to the initial consumption of copper-ammonia complex upon mixing with sodium thiosulfate solution, leading to lower concentrations in the 0.30 mol/L groups due to higher consumption rates from the increased sodium thiosulfate concentration. Moreover, the decreasing trend in copper-ammonia complex concentration was slower in the 0.15 mol/L group compared to the 0.30 mol/L group, indicating a slower reaction rate for Reaction 1 due to lower thiosulfate concentration. After 30 min, the copper-ammonia complex concentrations in the 0.15 mol/L groups were reduced by 0.0116 mol/L and 0.0104 mol/L, while those in the 0.30 mol/L groups were reduced by 0.0176 mol/L and 0.0159 mol/L, respectively, indicating gradual concentration decreases over time, with higher thiosulfate concentrations leading to faster reduction rates. Additionally, magnetization treatment accelerated the reduction rates, highlighting its contribution to enhancing the reaction rate outlined in Equation (8) and the overall chemical activity of the sodium thiosulfate lixiviant solution.

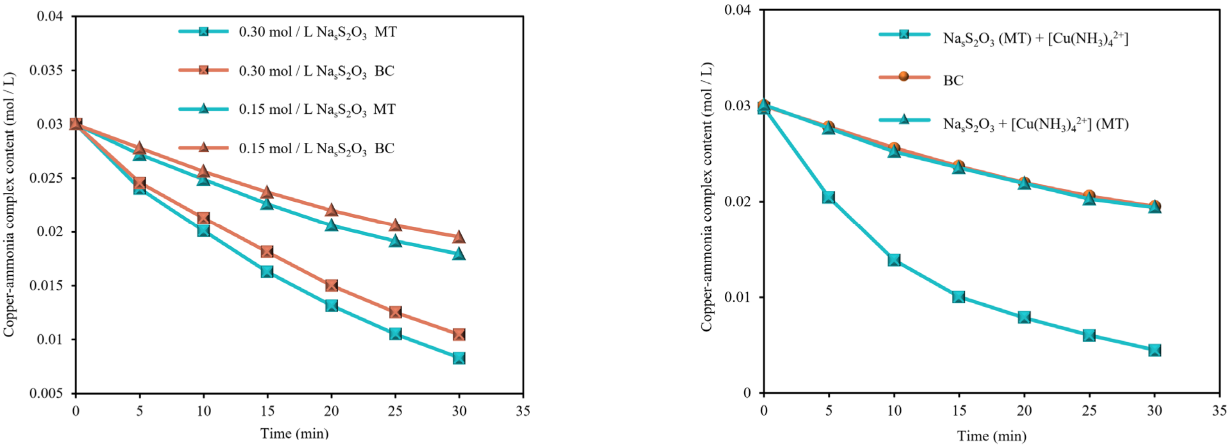

(**a**) (**b**)

Figure 5. Variation of copper-ammonia complex concentration in lixiviant solutions after magnetization treatment: (**a**) magnetizing sodium thiosulphate and copper-ammonia complexes synchronously; (**b**) magnetizing sodium thiosulphate and copper-ammonia complexes individually.

Subsequently, the separate magnetization of copper-ammonia complex and sodium thiosulfate followed by their combination into the lixiviant solution elucidated which component was predominantly enhanced by magnetization. The results in Figure 5b demonstrate that while the concentration and trends of copper-ammonia complex remained consistent in the magnetized sodium thiosulfate solution and unmagnetized control groups, magnetization notably accelerated the reduction in copper-ammonia complex concentration when applied solely to the copper-ammonia complex component. Specifically, the concentration of copper-ammonia complex reduced from 0.0253 mol/L to 0.0045 mol/L after 30 min of static treatment, emphasizing the heightened chemical reactivity and promotion of Equation (8) facilitated by magnetization.

3.2.3. Leaching Rate

This section utilized QCM-D to assess the mass change of gold-plated quartz resonator before and after magnetization treatment of the lixiviant solution, aiming to explore the impact of magnetization on the rate of gold leaching with sodium thiosulfate.

Figure 6a presents the frequency change Δf, energy dissipation change ΔD (Figure 6b), and mass change Δm (Figure 6c) over time. From Figure 6a, it is evident that Δf increases immediately upon the introduction of sodium thiosulfate gold leaching solution, signifying the commencement of the reaction between the solution and gold. Δf exhibits a linear increase over time, indicating a proportional relationship with leaching duration. Notably, Δf rises more rapidly post-magnetization of the sodium thiosulfate lixiviant solution. Upon introducing ultrapure water into the system, the rate of Δf increase gradually decelerates, stabilizing at 12,274 Hz for the magnetized group and 11,670 Hz for the unmagnetized group. This stability suggests irreversible reaction completion between sodium thiosulfate lixiviant solution and gold, with a higher leaching extent observed in the magnetized group.

From Figure 6b, after the lixiviant solution passage, the resonator's resistance to vibration abruptly rises, leading to a sharp increase in ΔD. The magnetized group exhibits higher ΔD values, attributed to the orderly molecular arrangement in the magnetized solution creating increased resistance to resonator vibration. Over time, the magnetized group reaches a peak ΔD of 11.81 ppm, while the unmagnetized group peaks at 11.03 ppm. Post-flushing with ultrapure water, the stabilized magnetized group records a ΔD of 7.71 ppm, significantly higher than the unmagnetized group's 2.24 ppm. This difference arises from increased surface roughness of the resonator's gold plating layer due to solution-induced corrosion, leading to higher energy loss during vibration cycles in the magnetized group.

The mass variation curves Δm vs. time t obtained from the Saurbray model in Figure 6c depict the gradual corrosion of the gold-plated layer by the lixiviant solution, resulting in linear mass reduction over time. This aligns with conclusions from Figure 6a, highlighting a first-order linear increase in gold leaching rate with leaching time. Post-ultrapure water flushing, the final gold leaching mass for the magnetized group is 24,747.70 ng, compared to 23,568.31 ng for the unmagnetized group. The gold leaching rate of the magnetized group (1637.53 ng/(cm^2·min)) surpasses that of the unmagnetized group (1561.39 ng/(cm^2·min)), affirming that magnetization accelerates the sodium thiosulfate leaching solution's chemical reaction rate with gold.

In summary, Δf and Δm curves demonstrate that magnetization effectively enhances the gold leaching rate, with the magnetized group exhibiting a higher leaching reaction degree under equivalent leaching times. The ΔD curve indicates significantly higher surface roughness of the magnetized group's gold layer compared to the non-magnetized group, further corroborating that magnetization catalyzes the copper-ammonia sodium thiosulfate leaching reaction of gold.

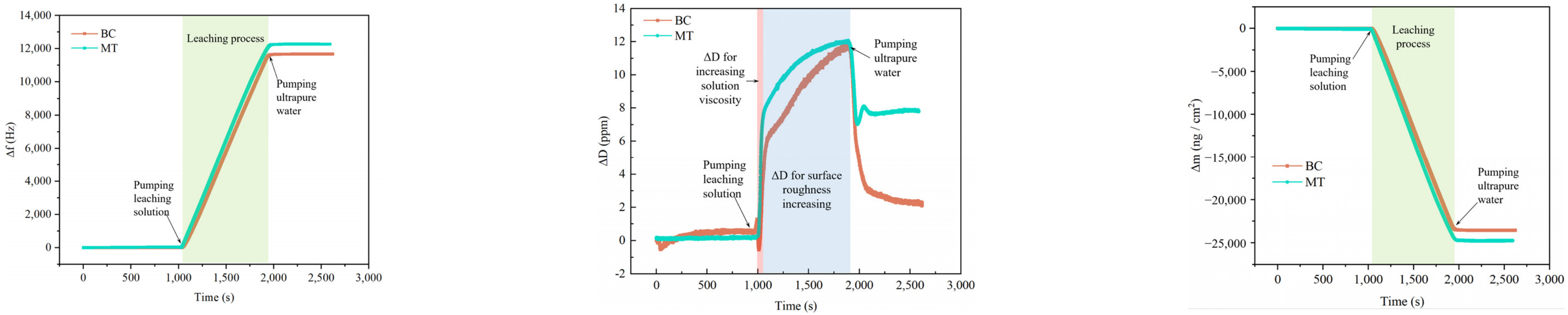

(**a**) (**b**) (**c**)

Figure 6. QCMD test results: (**a**) variation of frequency change Δf over time; (**b**) Variation of energy dissipation change ΔD over time; (**c**) variation of mass change Δm over time.

3.2.4. Contact Angle

Previous research has demonstrated that magnetization has a positive impact on surface tension, dissolved oxygen (DO) content, the reactivity of copper-ammonia complexes, and the rate of the copper-ammonia thiosulfate gold leaching reaction. Building upon these findings, it becomes apparent that magnetization can expedite the kinetic process involved in the copper-ammonia thiosulfate gold leaching reaction. This section focuses on investigating four shrinking core models (represented by Equations (10)–(13)) to ascertain the rate-controlling factor and the underlying nature of the gold dissolution process using copper-ammonia thiosulfate lixiviant.

Equation (10) is applied to a film diffusion-controlled process; Equation (11) is a chemical reaction-controlled process; Equation (12) is a product layer diffusion-controlled process and Equation (13) is a mixed-controlled process (a combination of intraparticle diffusion and chemical reaction).

$$\mathrm{x} = \mathrm{k_1 t} \tag{10}$$

$$1 - \left(1 - \mathrm{x}\right)^{\frac{1}{3}} = \mathrm{k_2 t} \tag{11}$$

$$1 - \frac{2}{3}\mathrm{x} - \left(1 - \mathrm{x}\right)^{\frac{2}{3}} = \mathrm{k_3 t} \tag{12}$$

$$\frac{\ln(1 - \mathrm{x})}{3} + \left[(1 - \mathrm{x})^{\frac{1}{3}} - 1\right] = \mathrm{k_4 t} \tag{13}$$

The gold extraction data from the copper-ammonia thiosulfate gold leaching reaction were gathered and fitted using the above equations. The fitting outcomes are depicted in Figure 7. The results reveal that the leaching reaction of copper-ammonia thiosulfate solution with gold foil conforms to both the film diffusion-controlled process model and the chemical reaction-controlled process. Notably, the fitting degree for both the magnetized and unmagnetized groups exceeds 0.999. Furthermore, the surface rate constant of the magnetized group surpasses that of the unmagnetized group. This indicates that while the magnetization treatment does not alter the kinetic model of the copper-ammonia sodium thiosulfate lixiviant solution for gold leaching, it does enhance the reaction rate.

The leaching rate of gold from sodium thiosulfate leaching solution is influenced by both film diffusion and chemical reaction. Thus, to enhance the leaching rate of gold, it is crucial to improve both the diffusion rate of molecules in the solution and the reaction activity. The magnetization treatment accomplishes this by enhancing the infiltration characteristics of the leaching solution, thereby improving the diffusion rate, and also by enhancing the reaction activity of dissolved oxygen (DO) and copper-ammonia complex. This indicates that the magnetization treatment effectively enhances both the rate of external diffusion and the chemical reaction, consequently improving the overall rate of the gold-leaching reaction.

In summary, the rate of the copper-ammonia thiosulfate gold leaching reaction is primarily influenced by the film diffusion process and the chemical reaction process. The magnetization treatment boosts the leaching rate from both of these perspectives. On one hand, the magnetization treatment significantly affects the wettability of the gold ore, as evidenced by the reduced surface tension of the lixiviant solution by 3.71 mN/m and the decreased contact angle by 3.20°. These reductions effectively promote the external diffusion process of the gold-leaching reaction. On the other hand, the magnetized leaching solution exhibits increased DO content and improved reactivity of the copper-ammonia complex, leading to enhanced chemical reaction processes in the leaching reaction. Therefore, from a kinetic mechanism perspective, the magnetization treatment reinforces the reaction process of copper-ammonia sodium thiosulfate gold leaching.

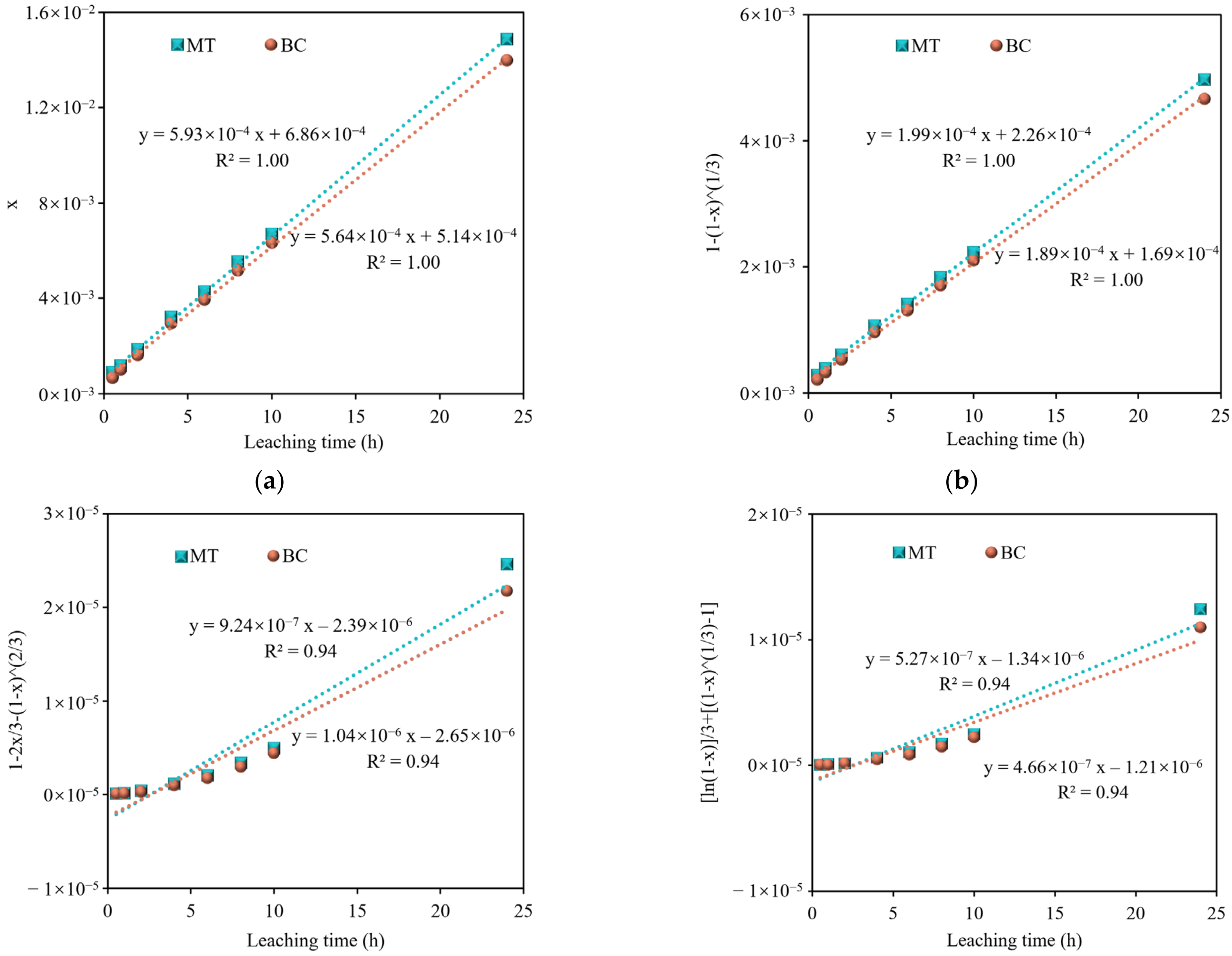

(**a**) (**b**)

(**c**) (**d**)

Figure 7. Gold leaching fitting with four control models: (**a**) film diffusion-controlled process; (**b**) chemical reaction-controlled process; (**c**) product layer diffusion-controlled process; (**d**) mixed-controlled process.

3.3. Column Leaching

Column leaching is a widely used method to simulate heap leaching processes, allowing for the investigation of the impact of magnetization treatment on gold-leaching reactions using copper-ammonia sodium thiosulfate. Figure 8 illustrates the variations in leaching rate (daily gold extraction) and gold extraction over time.

From Figure 8a, the daily leaching rate curves for both the magnetized and unmagnetized groups exhibit a similar pattern of gradual decrease, sharp decrease, and subsequent slow decrease. The higher leaching rate in the magnetized group is primarily observed in the initial 8 days, while in the unmagnetized group, it spans the first 9 days. This higher initial leaching rate is attributed to the preferential leaching of bare gold. The leaching kinetics indicate that sodium thiosulfate leaching rates are jointly determined by external diffusion and chemical reaction. During the pre-column leaching phase, molecules/ions in the lixiviant solution readily diffuse to the surface of bare gold, resulting in faster leaching due to initial contact and reaction. For instance, the leaching rate on the first day was 4.08%/d for the magnetized group and 3.42%/d for the unmagnetized group. In the middle stage of column leaching, as bare gold diminishes, semi-bared and fissured gold becomes the main leaching target, emphasizing external diffusion over chemical reaction. By-products like sulfur monomers and copper sulfide may hinder leaching solution infiltration, leading to a decrease in the leaching rate for both groups.

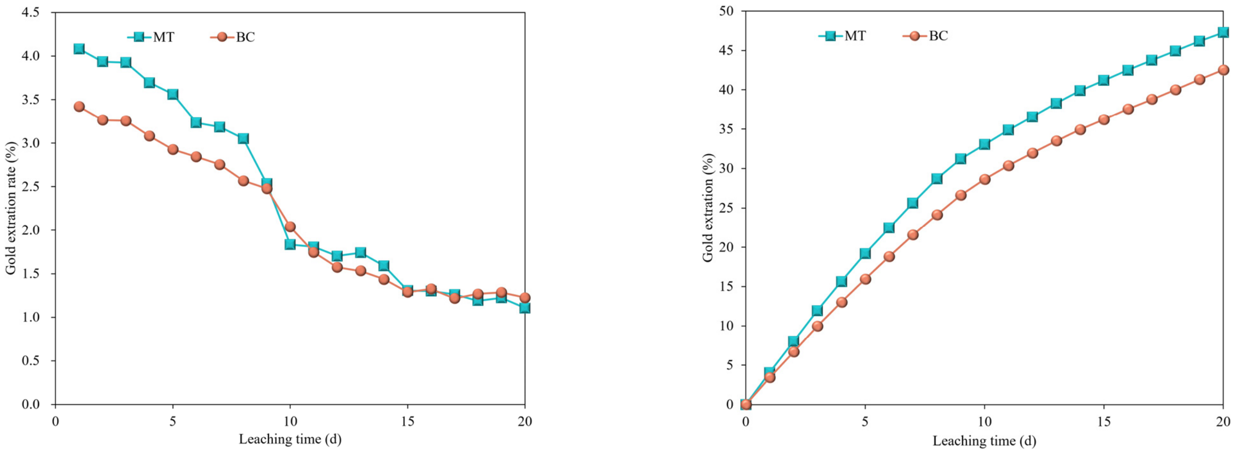

(**a**) (**b**)

Figure 8. Gold extraction over time: (**a**) daily extraction; (**b**) cumulative extraction.

In the late stage of column leaching, with the majority of bare gold leached, semi-bared and fissured gold dominates the leaching process, further accentuating external diffusion. The leaching rate of the unmagnetized group surpassed that of the magnetized group on the 18th day, with rates of 1.22%/d and 1.10%/d on the 20th day for each group, respectively. This reversal in leaching rates is attributed to higher recoverable gold in the magnetized group during the later stages. The average daily leaching rate was 2.36%/d for the magnetized group and 2.13%/d for the unmagnetized group, reflecting the earlier findings regarding improved infiltration characteristics and chemical reaction acceleration due to magnetization.

In Figure 8b, the gold extraction curve shows a final extraction rate of 47.27% for the magnetized group, 42.53% for the unmagnetized group, and 43.60% for cyanidation-based column leaching (cyanide lixiviant solution concentration is 300 ppm, pH ranges from 10.5 to 11, and dripping intensity is 6 L/(m^2·h)). Magnetization treatment led to a 4.74% increase in gold recovery compared to the unmagnetized group and a 3.67% increase compared to cyanidation. This demonstrates the effectiveness of magnetization treatment in enhancing the leaching effect of copper-ammonia thiosulfate, aligning with previous research findings and suggesting potential for replacing cyanidation in heap leaching methods.

4. Conclusions

(1) Under optimized conditions including a magnetic field strength of 1.5 T, magnetization time of 5 min, and liquid flow rate of 1000 mL/min, the surface tension of sodium thiosulphate lixiviant solution decreased by 3.71 mN/m, representing a 5.5% reduction. Magnetization can increase the dissolved oxygen in the sodium thiosulphate lixiviant solution by up to 38%.

(2) The magnetization treatment significantly improved the infiltration characteristics of the leaching solution on gold ore, reducing the contact angle from 75.54° to 73.24°. Moreover, it enhanced the reactivity of copper-ammonia complexes and improved the leaching reaction. Based on QCMD leaching rate tests, the magnetization treatment increased the reaction rate of copper-ammonia sodium thiosulphate leaching from 1561.39 ng/cm^2-min to 1637.53 ng/cm^2-min, a 4.88% increase.

(3) Leaching kinetics studies reveal that the reaction rate of gold leaching with sodium copper-ammonia thiosulphate is determined by external diffusion and chemical reaction processes. Magnetization improves the infiltration characteristics of the leaching solution, aiding the diffusion of molecules/ions onto gold surfaces and enhancing external diffusion rates. Additionally, it boosts the activity of copper-ammonia complexes and DO in the leaching solution, thereby improving the chemical reaction process of gold leaching. Hence, magnetization treatment effectively increases the

leaching reaction rate, although further research is needed to elucidate the detailed mechanisms, particularly regarding the enhancement of copper-ammonia complex activity post-magnetization.

(4) Magnetization significantly enhanced heap leaching with copper-ammonia sodium thiosulphate, increasing the leaching rate by approximately 0.6%. The reaction rate in the early stage is primarily driven by external diffusion and chemical reaction processes, with bare gold as the primary reactant. In the middle and late stages, the increase in leaching reaction by-products obstructs the external diffusion process, leading to a sharp decrease in reaction rate. The cumulative extraction rate for the copper-ammonia sodium thiosulphate magnetized group reached 47.27%, with magnetization treatment enhancing the gold leaching rate by 4.74% and 3.67% compared to the blank control group and cyanide leaching, respectively, indicating the potential of magnetization treatment in promoting the industrial use of sodium thiosulphate as an alternative to cyanide for gold leaching.

This study illustrates that magnetization can indeed amplify the chemical reactivity of copper-ammonia complexes, albeit not sodium thiosulfate. However, the mechanism underlying how magnetization enhances the activation of gold leach molecules remains unclear. Therefore, employing molecular simulation is anticipated to delve into the structural and property alterations of copper-ammonia complexes post-magnetization.

Author Contributions: Conceptualization, Z.L. and J.K.; methodology, J.K.; software, L.F.; validation, J.K., W.Z. and J.T.; formal analysis, Z.L.; investigation, C.S.; resources, Q.L.; data curation, J.L.; writing—original draft preparation, Z.L. and L.F.; writing—review and editing, C.S. and L.F.; visualization, C.X.; supervision, G.L.; project administration, J.K.; funding acquisition, J.K. All authors have read and agreed to the published version of the manuscript.

Funding: This research was funded by the Natural Science Foundation of China (NSFC), No. 51974016.

Data Availability Statement: The experimental data used to support the findings of this study are included in the manuscript.

Acknowledgments: The authors gratefully acknowledge the editors and reviewers who put their efforts on this manuscript.

Conflicts of Interest: Lipeng Fan is employed by Ansteel Group Mining Company Ltd., Weibin Zhang, Qiang Li, Jiubo Liu, Chengjun Xing and Guanhua Li are employed by China National Gold Group Inner Mongolia Taiping Mining Co., Ltd., Jie Tian is employed by Engineering Company of Beijing General Research Institute of Mining and Metallurgy Technology Group. The paper reflects the views of the scientists and not the companies.

References

1. Bas, A.D.; Koc, E.; Yazici, E.Y.; Deveci, H. Treatment of copper-rich gold ore by cyanide leaching, ammonia pretreatment and ammoniacal cyanide leaching. *Trans. Nonferrous Met. Soc.* **2015**, *25*, 597–607. [CrossRef]
2. Dong, K.; Xie, F.; Wang, W.; Chang, Y.; Chen, C.; Gu, X. Efficient destruction of sodium cyanide by thermal decomposition with addition of ferric oxide. *Trans. Nonferrous Met. Soc.* **2021**, *31*, 1113–1126. [CrossRef]
3. Li, K.; Li, Q.; Jiang, T.; Yang, Y.; Xu, B.; Xu, R.; Zhang, Y. Thiourea leaching of gold in presence of jarosite and role of oxalate. *Trans. Nonferrous Met. Soc.* **2024**, *34*, 322–335. [CrossRef]
4. Yin, S.; Wang, L.; Chen, X.; Wu, A. Effect of ore size and heap porosity on capillary process inside leaching heap. *Trans. Nonferrous Met. Soc.* **2016**, *26*, 835–841. [CrossRef]
5. Li, G.; Kou, J.; Xing, Y.; Hu, Y.; Han, W.; Liu, Z.; Sun, C. Gold-leaching performance and mechanism of sodium dicyanamide. *Int. J. Min. Met. Mater.* **2021**, *28*, 1759–1768. [CrossRef]
6. Ou, Y.; Yang, Y.; Li, K.; Gao, W.; Wang, L.; Li, Q.; Jiang, T. Eco-friendly and low-energy innovative scheme of self-generated thiosulfate by atmospheric oxidation for green gold extraction. *J. Clean. Prod.* **2023**, *387*, 135818. [CrossRef]
7. Örgül, S.; Atalay, Ü. Reaction chemistry of gold leaching in thiourea solution for a Turkish gold ore. *Hydrometallurgy* **2022**, *67*, 71–77. [CrossRef]
8. Wu, H.; Feng, Y.; Li, H.; Li, H.; Ju, J. Effect of sodium carbonate on alkaline self-leaching of gold from flotation gold ore. *Sep. Purif. Technol.* **2021**, *256*, 117499. [CrossRef]

9. Liu, W.; Yang, T.; Xia, X. Behavior of silver and lead in selective chlorination leaching process of gold-antimony alloy. *Trans. Nonferrous Met. Soc.* **2010**, *20*, 322–329. [CrossRef]
10. Konyratbekova, S.S.; Baikonurova, A.; Ussoltseva, G.A.; Erust, C.; Akcil, A. Thermodynamic and kinetic of iodine–iodide leaching in gold hydrometallurgy. *Trans. Nonferrous Met. Soc.* **2015**, *25*, 3774–3783. [CrossRef]
11. Yin, X.; Liu, R.; Cheng, M.; Sun, Q.; Yang, Y. Efficient leaching and recovery of metallic gold and copper from integrated circuits with the novel bromotrihalide ionic liquids based on the redox mechanism. *Sep. Purif. Technol.* **2023**, *313*, 123456. [CrossRef]
12. Sarvar, M.; Shafaei, Z.T.; Noaparast, M.; Badiei, A.R.; Amiri, A. Application of amino acids for gold leaching: Effective parameters and the role of amino acid structure. *J. Clean. Prod.* **2023**, *391*, 136123. [CrossRef]
13. Qin, X.; Zhang, T.; Zi, F.; Zang, H.; Li, G. Study on Synergistic Strengthening of Gold Extraction with Copper Ethylenediamine Thiosulfate Using Pyrite and Nickel Ions. *Minerals* **2024**, *14*, 2. [CrossRef]
14. Baghalha, M. Leaching of an oxide gold ore with chloride/hypochlorite solutions. *Int. J. Min. Process* **2007**, *82*, 178–186. [CrossRef]
15. Sronsri, C.; Sittipol, W.; Panitantum, N. Enhanced and selective gold recovery from phone waste: Use of thiosulfate, dissolved oxygen, and an agriculture-based, low-cost adsorbent. *Hydrometallurgy* **2023**, *220*, 106108. [CrossRef]
16. Zhao, H.; Yang, H.; Zhang, Q.; Tong, L.; Jin, Z.; Chen, G. Research status of factors influence on leaching of gold with thiosulfate. *Gol. Sci. Technol.* **2018**, *26*, 105–114.
17. Zhang, X.; Senanayake, G. A Review of Ammoniacal Thiosulfate Leaching of Gold: An Update Useful for Further Research in Non-cyanide Gold Lixiviants. *Miner. Process. Extr. Metall. Rev.* **2016**, *37*, 385–411. [CrossRef]
18. Senanayake, G. Analysis of reaction kinetics, speciation and mechanism of gold leaching and thiosulfate oxidation by ammoniacal copper(II) solutions. *Hydrometallurgy* **2004**, *75*, 55–75. [CrossRef]
19. Aylmore, M.G.; Muir, D.M. Thiosulfate leaching of gold—A review. *Min. Eng.* **2001**, *14*, 135–174. [CrossRef]
20. Senanayake, G. Gold leaching in non-cyanide lixiviant systems: Critical issues on fundamentals and applications. *Min. Eng.* **2004**, *17*, 785–801. [CrossRef]
21. Lin, Y.; Hu, X.; Zi, F.; Chen, Y.; Chen, S.; Li, X.; Zhao, L.; Li, Y. Synergistical thiourea and thiosulfate leaching gold from a gold concentrate calcine with copper-ammonia catalysis. *Sep. Purif. Technol.* **2023**, *327*, 124928. [CrossRef]
22. Jeffrey, M.I. Kinetic aspects of gold and silver leaching in ammonia–thiosulfate solutions. *Hydrometallurgy* **2001**, *60*, 7–16. [CrossRef]
23. Zhang, G.; Hou, L.; Chen, P.; Zhang, Q.; Chen, Y.; Zainiddinovich, N.Z.; Wu, C.; Alejandro, L.V.; Jia, F. Efficient and stable leaching of gold in a novel ethydiaminedhephen acetic-thiosulfate system. *Min. Eng.* **2024**, *209*, 108639. [CrossRef]
24. Mahandra, H.; Faraji, F.; Ghahreman, A. Novel Extraction Process for Gold Recovery from Thiosulfate Solution Using Phosphonium Ionic Liquids. *Acs Sustain. Chem. Eng.* **2021**, *9*, 8179–8185. [CrossRef]
25. Guo, H.; Wang, S.; Nie, Y.; Chen, J.; Wang, Q. Improving the cementation effect of copper on gold in thiosulfate solution by pre-regulating the existing form of Cu^{2+}. *J. Ind. Eng. Chem.* **2024**, *130*, 483–493. [CrossRef]
26. Wang, J.; Wang, R.; Pan, Y.; Liu, F.; Xu, Z. Thermodynamic analysis of gold leaching by copper-glycine-thiosulfate solutions using Eh-pH and species distribution diagrams. *Min. Eng.* **2022**, *179*, 107438. [CrossRef]
27. Chen, J.; Xie, F.; Wang, W.; Fu, Y.; Wang, J. Leaching of a carbonaceous gold concentrate in copper-tartrate-thiosulfate solutions. *Miner. Eng.* **2022**, *183*, 107605. [CrossRef]
28. Moosavi, F.; Gholizadeh, M. Magnetic effects on the solvent properties investigated by molecular dynamics simulation. *J. Magn. Magn. Mater.* **2014**, *354*, 239–247. [CrossRef]
29. Toledo, E.J.L.; Ramalho, T.C.; Magriotis, Z.M. Influence of magnetic field on physical–chemical properties of the liquid water: Insights from experimental and theoretical models. *J. Mol. Struct.* **2008**, *888*, 409–415. [CrossRef]
30. Wang, Y.; Wei, H.; Li, Z. Effect of magnetic field on the physical properties of water. *Results Phys.* **2018**, *8*, 262–267. [CrossRef]
31. Wang, Y.; Zhang, B.; Gong, Z.; Gao, K.; Ou, Y.; Zhang, J. The effect of a static magnetic field on the hydrogen bonding in water using frictional experiments. *J. Mol. Struct.* **2013**, *1052*, 102–104. [CrossRef]
32. Lee, H.S.; Yap, A.C.W.; Ng, C.C.; Mohd, N.S.; Loo, J.L. Increased electron density and dissolved oxygen level in water through magnetic effect. In Proceedings of the 9th International Conference on Future Environment and Energy, Osaka, Japan, 9–11 January 2019.
33. Zheng, Y.; Hao, Z.; Wang, X.; Qiao, J.; Li, X. Study on effect of magnetization on wetting characteristics of water with different ions to coal dust. *Fuel* **2024**, *367*, 131441. [CrossRef]
34. Al-Akhras, M.A.H.; Al-Quraan, N.A.; Abu-Aloush, Z.A.; Mousa, M.S.; AlZoubi, T.; Makhadmeh, G.N.; Donmez, O.; Aljarrah, K. Impact of magnetized water on seed germination and seedling growth of wheat and barley. *Results Eng.* **2024**, *22*, 101991. [CrossRef]
35. Keshta, M.M.; Elshikh, M.M.Y.; Kaloop, M.R.; Hu, J.; Elmohsen, I.A. Effect of magnetized water on characteristics of sustainable concrete using volcanic ash. *Constr. Build. Mater.* **2022**, *361*, 129640. [CrossRef]
36. Gao, F.; Zheng, Y.; Li, J.; Lu, N.; Yin, Y.; Jia, H.; Wang, J. Magnetization coupled reverse osmosis (RO): Enhanced inhibition scaling mechanisms and operation optimization. *Chem. Eng. Sci.* **2024**, *286*, 119650. [CrossRef]
37. Pang, J.; Xie, J.; Zhao, Z.; Hao, Y.; Han, Q.; Liang, L. Study on improving the wettability of anthracite dust by surfactant-magnetized water. *Trans. Beijing Inst. Technol.* **2021**, *44*, 83–90.
38. Zhou, Q.; Qin, B.; Huang, H. Research on the formation mechanism of magnetized water used to wet coal dust based on experiment and simulation investigation on its molecular structures. *Powder Technol.* **2021**, *391*, 69–76. [CrossRef]

39. Amiri, M.C.; Dadkhah, A.A. On reduction in the surface tension of water due to magnetic treatment. *Colloids Surf. A* **2006**, *278*, 252–255. [CrossRef]
40. Sronsri, C.; U-yen, K.; Sittipol, W. Analyses of vibrational spectroscopy, thermal property and salt solubility of magnetized water. *J. Mol. Liq.* **2023**, *323*, 114613. [CrossRef]
41. Rong, X.; Li, J.; Dan, H.; Xue, C.; Gao, M.; Li, M.; Liu, Y. Characteristics, Mechanism and Applications of Magnetized Water: A Review. *Mater. Rep.* **2022**, *36*, 21020032-7.
42. Huminic, G.; Huminic, A.; Vărdaru, A.; Fleacă, C.; Dumitrache, F.; Morjan, I. Surface tension of Ag NPs-rGO based hybrid nanofluids. *J. Mol. Liq.* **2023**, *390*, 123002. [CrossRef]
43. *GB/T20899.1-2019*; Methods for Chemical Analysis of Gold Ores—Part 1: Determination of Gold Content. National Public Service Platform for Standards Information: Beijing, China, 2019.